

Original Article  
Anatomy/Histology/  
Embryology



# Morphology of the aortic arch branching pattern in raccoon dogs (*Nyctereutes procyonoides*, Gray, 1834)

Euiyong Lee <sup>1</sup>, Young-Jin Jang <sup>1</sup>, In-Shik Kim <sup>1</sup>, Hyun-Jin Tae <sup>1</sup>,  
Jeoungha Sim <sup>2,\*</sup>, Dongchoon Ahn <sup>1,\*</sup>

<sup>1</sup>Department of Veterinary Medicine, College of Veterinary Medicine and Institute of Animal Transplantation, Jeonbuk National University, Iksan 54596, Korea

<sup>2</sup>Department of Nursing, College of Medical Science, Jeonju University, Jeonju 55069, Korea

 OPEN ACCESS

Received: Dec 3, 2023

Revised: Jan 21, 2024

Accepted: Feb 12, 2024

Published online: Mar 14, 2024

\*Corresponding authors:

Jeoungha Sim

Department of Nursing, College of Medical Science, Jeonju University, 303 Cheonjam-ro, Wansan-gu, Jeonju 55069, Korea.

Email: jha880@jj.ac.kr

<https://orcid.org/0000-0003-1307-8010>

Dongchoon Ahn

Department of Veterinary Medicine, College of Veterinary Medicine and Institute of Animal Transplantation, Jeonbuk National University, 79 Gobong-ro, Iksan 54596, Korea.

Email: ahndc@jbnu.ac.kr

<https://orcid.org/0000-0002-7024-1606>

## ABSTRACT

**Background:** Aortic arch (AA) branching patterns vary among different mammalian species. Most previous studies have focused on dogs, whereas those on raccoon dogs remain unexplored.

**Objectives:** The objective of this study was to describe the AA branching pattern in raccoon dogs and compare their morphological features with those of other carnivores.

**Methods:** We prepared silicone cast specimens from a total of 36 raccoon dog carcasses via retrograde injection through the abdominal aorta. The brachiocephalic trunk (BCT) branching patterns were classified based on the relationship between the left and right common carotid arteries. The subclavian artery (SB) branching pattern was examined based on the order of the four major branches: the vertebral artery (VT), costocervical trunk (CCT), superficial cervical artery (SC), and internal thoracic artery (IT).

**Results:** In most cases (88.6%), the BCT branched off from the left common carotid artery and terminated in the right common carotid and right subclavian arteries. In the remaining cases (11.4%), the BCT formed a bicarotid trunk. The SB exhibited various branching patterns, with 26 observed types. Based on the branching order of the four major branches, we identified the main branching pattern, in which the VT branched first (98.6%), the CCT branched second (81.9%), the SC branched third (62.5%), and the IT branched fourth (52.8%).

**Conclusions:** The AA branching pattern in raccoon dogs exhibited various branching patterns with both similarities and differences compared to other carnivores.

**Keywords:** Aortic arch; brachiocephalic trunk; raccoon dogs; subclavian artery; branching pattern

## INTRODUCTION

Aortic arch (AA) branching patterns represent diverse variations among mammalian species, including carnivores [1-3], rodents [4,5], primates [6], pigs [7], horses [8], and ruminants [9-11]. Each species has distinctive features [12].

© 2024 The Korean Society of Veterinary Science

This is an Open Access article distributed under the terms of the Creative Commons Attribution Non-Commercial License (<https://creativecommons.org/licenses/by-nc/4.0>) which permits unrestricted non-commercial use, distribution, and reproduction in any medium, provided the original work is properly cited.

**ORCID iDs**

Euiyong Lee  
<https://orcid.org/0000-0001-9602-1583>  
 Young-Jin Jang  
<https://orcid.org/0000-0002-0898-373X>  
 In-Shik Kim  
<https://orcid.org/0000-0003-1767-5795>  
 Hyun-Jin Tae  
<https://orcid.org/0000-0002-5193-508X>  
 Jeoung-ha Sim  
<https://orcid.org/0000-0003-1307-8010>  
 Dongchoon Ahn  
<https://orcid.org/0000-0002-7024-1606>

**Author Contributions**

Conceptualization: Ahn D, Sim J; Formal analysis: Lee E, Jang YJ, Ahn D; Funding acquisition: Ahn D; Investigation: Lee E, Jang YJ; Methodology: Lee E; Project administration: Sim J, Ahn D; Resources: Ahn D, Kim IS, Tae HJ; Software: Lee E, Jang YJ; Supervision: Sim J, Kim IS, Ahn D; Validation: Kim IS, Tae HJ; Visualization: Lee E, Jang YJ; Writing - original draft: Lee E, Jang YJ; Writing - review & editing: Lee E, Jang YJ, Kim IS, Sim J, Ahn D.

**Conflict of Interest**

The authors declare no conflicts of interest.

**Funding**

This research was supported by a grant from the National Research Foundation of Korea (NRF), funded by the Ministry of Science and ICT (MSIT), Government of the Republic of Korea (grant number: NRF-2019R1I1A3A01064272).

In anatomical textbooks, representative types of AA branching patterns for carnivores are illustrated using dogs as examples. In dogs, the AA divides into two arteries, namely the brachiocephalic trunk (BCT) and left subclavian artery (LSB). The BCT further branches into the left common carotid artery (LCC), right common carotid artery (RCC), and right subclavian artery (RSB) [13-17].

However, this description does not reflect the diversity of AA branching patterns in carnivores. For instance, in some marine species, such as the gray seal [12], deep-diving hooded seal [18], and ringed seal [19], the AA branches into three arteries: the BCT, LCC, and LSB. Moreover, studies on dogs [20], cats [3,21], and Eurasian otters [2] found intraspecific variations based on the configuration between the LCC and RCC. The bicarotid trunk (BC) has been reported in various carnivorous species, including dogs [20], cats [21], crab-eating foxes [22], Eurasian otters [2], racoons [12], and giant pandas [23].

The subclavian artery (SB) also exhibits various branching patterns in carnivores [1,2,24,25]. The SB branches into four arteries: the vertebral artery (VT), costocervical trunk (CCT), superficial cervical artery (SC), and internal thoracic artery (IT) [13-16]. However, the specific branching sequences of these four arteries are not detailed in most textbooks [13-15,26]. Some textbooks state that the VT and CCT are typically the first and second branches, respectively [17,27,28].

However, studies on SB branching patterns have reported a wide variation in dogs [1,25], cats [29], and Eurasian otters [2]. These variations make it challenging to determine the typical branching sequences of the four arteries. Particularly in cats [29] and Eurasian otters [2], it has been frequently observed that the IT branches as one of the first two arteries. These findings suggest the need for comprehensive and comparative anatomical studies of SB branching patterns.

Therefore, to further investigate AA branching patterns in carnivores, we decided to study raccoon dogs (*Nyctereutes procyonides*, Gray, 1834). Based on mitochondrial genome analyses, raccoon dogs show genetic affiliations with members of the Canidae family, especially with species from the genera *Canis*, *Chrysocyon*, *Cuon*, and *Vulpes* [30]. Recently, with an increase in the raccoon dog population, the importance of research on anatomical structures has grown [31]. However, limited research has been conducted on the arteries of raccoon dogs, including the basilar arteries of the brain [32], facial arteries [33], and middle cerebral arteries [34]. No reports have investigated the anatomical patterns and variations in the AA in raccoon dogs.

Based on existing knowledge, our study aimed to describe the AA branching pattern in raccoon dogs and compare their morphological features with those of other carnivores. This study contributes to our understanding of vascular anatomy and highlights interspecific variations.

## MATERIALS AND METHODS

### Samples

A total of 36 raccoon dog carcasses (14 males and 22 females) that died during rescue or care were obtained from the Jeonbuk Wildlife Rescue Center and Kangwon Wildlife Rescue Center for anatomical research. The Institutional Animal Care and Use Committee (IACUC) at Jeonbuk National University confirmed that ethical approval was not required for the use of animal carcasses in our study (pain category A; use of non-living tissues).

### Vascular casting

We prepared silicone casts to examine AA branching patterns, as previously described [9]. The thoracic and abdominal cavities were opened to expose the abdominal aorta. An incision was made cranial to the celiac artery in the abdominal aorta, and blood clots were flushed with saline. Commercial silicone (Lucky-Silicone; Wacker Chemical Korea, Korea) was injected retrogradely through the incision. After ensuring that the silicone had filled the major branches of the AA, the casts were left to solidify for 48 h. Subsequently, the casts were analyzed for their branching patterns and photographed. Due to the failure of one BCT cast, our study used 35 BCT casts and 72 SB casts.

### Symbols

AA branching patterns are represented by four symbols indicating the positional relationship between the two arterial branches (**Fig. 1**) [2]. “A-B” indicates that arteries A and B branched off in that order. “A≈B” indicates that arteries A and B branched at a similar level, whereas “[A=B]” indicates that arteries A and B branched at the same branching level. If the branching overlaps by more than half of the diameter of artery A, it is considered as “[A=B];” otherwise, it is “A≈B.” “[A&B]” indicates that arteries A and B arose from a common trunk.

### Classification of the AA branching patterns

The AA branching pattern was analyzed at three branching levels: AA, BCT, and SB. Each level applied a different classification method. All arteries were identified based on their distribution area, vascular route, and relationship with adjacent structures, as referenced from anatomical textbooks [15,17,35].

For the AA branching level, we classified the branching patterns according to the number of arteries branching off directly from the AA, referred to as AA-types [4]. In AA-type I, the AA only branched off one artery, the BCT. In AA-type II, the AA branched off two arteries, the BCT and LSB. In AA-type III, the AA gave off three arteries, the BCT, LCC, and LSB.

For the BCT branching level, we examined the branching pattern based on the relationship between the LCC, RCC, and RSB. These relationships are represented by the previously described symbols [2]. We measured the total length of the BCT (length A), the length from the AA to the LCC (length B), and the diameter of the LCC. The distance between the LCC and RCC branches (length C) was calculated by subtracting length B from length A. For BC, the distance from AA to BC was measured. Lengths A and B were measured from the

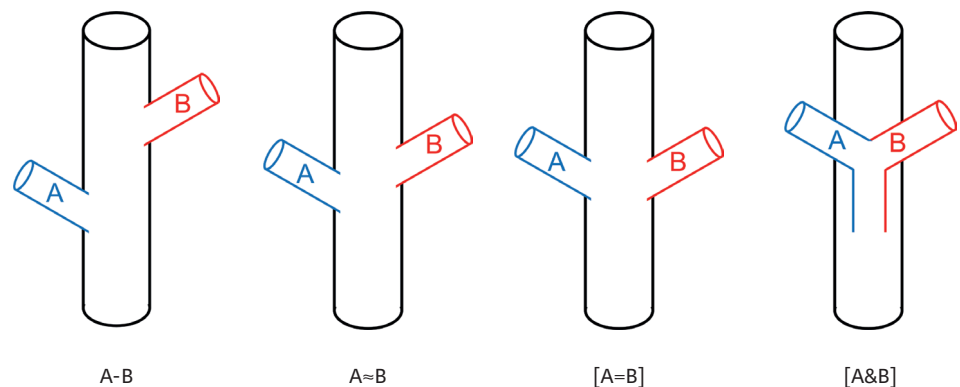


**Fig. 1.** Symbols representing the positional relationships between two arterial branches.

branching point of the BCT in the AA to the distal borders of RCC and LCC, respectively. Measurements were performed using digital Vernier calipers (Mitutoyo Co., Japan).

To further investigate the relationship between LCC and RCC, the ratio of the distance between the LCC and RCC to the total length of the BCT (RDCC, %) was calculated using the following formula:  $\text{Length C/Length A} \times 100$  (%). Based on the RDCC, four branching patterns were distinguished: RDCC-type I,  $\text{RDCC} > 30\%$ ; RDCC-type II,  $15\% < \text{RDCC} \leq 30\%$ ; RDCC-type III,  $0 < \text{RDCC} \leq 15\%$ ; and RDCC-type IV,  $\text{RDCC} = 0$  [2].

For the SB branching level, we examined the branching pattern based on the relationships between the four major branches: VT, CCT, IT, and SC. These relationships are represented by the previously described symbols. Branching patterns represented by the same symbol were categorized as a single pattern and referred to as the SB-type [2].

To further analyze the branching order of the four major branches, we counted the first, second, third, and fourth branches [2]. We determined the main branching pattern based on the branching order frequencies exceeding 50%. Additionally, we compared the frequencies of LSB and RSB, as well as between the sexes.

### Statistical analysis

All statistical analyses were performed using RStudio (version 2023.09.0+463; RStudio, USA). Data are presented as mean  $\pm$  SD. Differences in the numerical data were analyzed using the Student's *t*-test. The Mann-Whitney *U* test was used to assess differences in the arterial branching order in the SB, comparing individual arteries, between LSB and RSB, and between the sexes. Statistical significance ( $p < 0.05$ ) was determined.

## RESULTS

### Branching patterns at the branching level of the AA

We examined the AA branching patterns in raccoon dogs using silicone castings (**Fig. 2**). All 35 raccoon dogs showed AA-type II with two arteries, the BCT and LSB, branching from the AA. No anomalies were found in the AA of any raccoon dog.

### Branching patterns at the branching level of the BCT

We investigated the BCT branching patterns based on the relationships between the three major branches: LCC, RCC, and RSB. Among the 35 raccoon dogs, 31 had LCC-[RCC = RSB], where the LCC branched first and terminated in the RCC and RSB (88.6%). The remaining four animals displayed [[LCC&RCC] = RSB], in which LCC and RCC branched from a common trunk, known as the BC (11.4%).

We measured several BCT parameters from the silicone specimens. The mean length A was  $24.2 \pm 5.6$  mm, and the mean length B was  $19.9 \pm 4.7$  mm. The mean length C was  $4.4 \pm 2.6$  mm. RDCC values ranged from 0% to 38.3%, with a mean of  $17.5\% \pm 9.4\%$  (**Table 1**). The BCT branching patterns were classified into four types based on the RDCC. RDCC-type I was observed in four raccoon dogs (one male and three females; 11.4%). RDCC-type II was observed in 18 raccoon dogs (six males and 12 females; 51.4%). RDCC-type III was observed in nine raccoon dogs (four males, five females; 25.7%). Only four cases (two males and two females, 11.4%) exhibited an RDCC-type IV pattern with BC (**Fig. 3**).

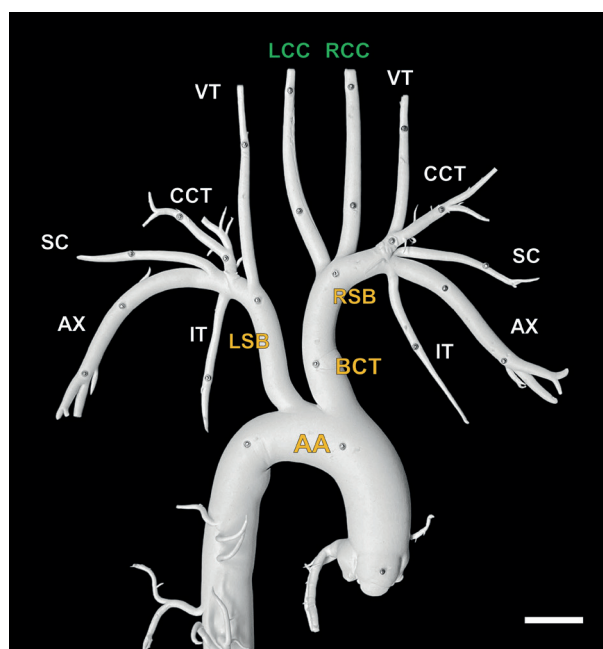


**Fig. 2.** Dorsal view of a silicone cast of the AA of a raccoon dog. Scale bar = 10 mm.

AA, aortic arch; BCT, brachiocephalic trunk; LSB, left subclavian artery; RSB, right subclavian artery; LCC, left common carotid artery; RCC, right common carotid artery; VT, vertebral artery; CCT, costocervical trunk; SC, superficial cervical artery; IT, internal thoracic artery; AX, axillary artery.

### Branching patterns at the branching level of the SB

We examined the SB branching patterns across a total of 72 cases in 36 raccoon dogs, including both LSB and RSB. Various SB branching patterns were observed in the 26 SB types from the total 72 cases (**Table 2, Fig. 4**). The most frequent SB-type was VT-CCT-SC-IT, which was found in 19 cases (26.4%). The second most prevalent SB-type was VT-CCT-[IT=SC], which was observed in 10 cases (13.9%). SB-types VT-CCT-IT-SC and VT-CCT-IT≈SC were observed in 5 cases (6.9%). The SB-type VT-[CCT=SC]-IT was observed in 4 cases (5.6%). Three SB-types, VT≈CCT≈SC-IT, VT-[CCT=IT]-SC, and [VT&CCT]-SC-IT, were each observed in three cases (4.2%). Two SB-types, VT-CCT-SC≈IT and VT-CCT≈SC-IT, were observed in two cases (2.8%). The remaining SB-types, represented by only one case each, constituted 1.4% of all cases.

We analyzed the branching order of the four major arteries of the SB (**Fig. 5**). The VT branched first in 71 (98.6%) and second in only one case (1.4%). The CCT branched first in 10 (13.9%), second in 59 (81.9%), and third in three cases (4.2%). The SC branched first in one (1.4%), followed by five (6.9%), 45 (62.5%), and 21 (29.2%) cases, respectively. The IT

**Table 1.** Average parameters of each type of the BCT in raccoon dogs

Parameters	RDCC-type I	RDCC-type II	RDCC-type III	RDCC-type IV	Total
Total length of BCT (length A) (mm)	27.2 ± 2.7	24.6 ± 6.2	24.4 ± 4.3	19.1 ± 6.0	24.2 ± 5.6
Length from AA to LCC (length B) (mm)	17.9 ± 2.1	19.7 ± 5.2	21.3 ± 3.8	19.1 ± 6.0	19.9 ± 4.7
Distance between LCC and RCC (length C) (mm)	9.3 ± 1.2	4.9 ± 1.4	3.1 ± 0.7	0	4.4 ± 2.6
Length of bicarotid trunk (mm)	-	-	-	3.6 ± 0.6	-
RDCC (Length C/Length A × 100) (%)	34.2 ± 3.2	20.1 ± 4.0	12.7 ± 1.9	0	17.5 ± 9.4
Diameter of LCC (mm)	3.2 ± 0.3	2.9 ± 0.7	2.8 ± 0.6	2.9 ± 0.6	2.9 ± 0.6

The data are presented as the mean ± SD.

RDCC, the ratio of the distance between the left and right common carotid arteries to the total length of the brachiocephalic trunk; BCT, brachiocephalic trunk; AA, aortic arch; LCC, left common carotid artery; RCC, right common carotid artery.

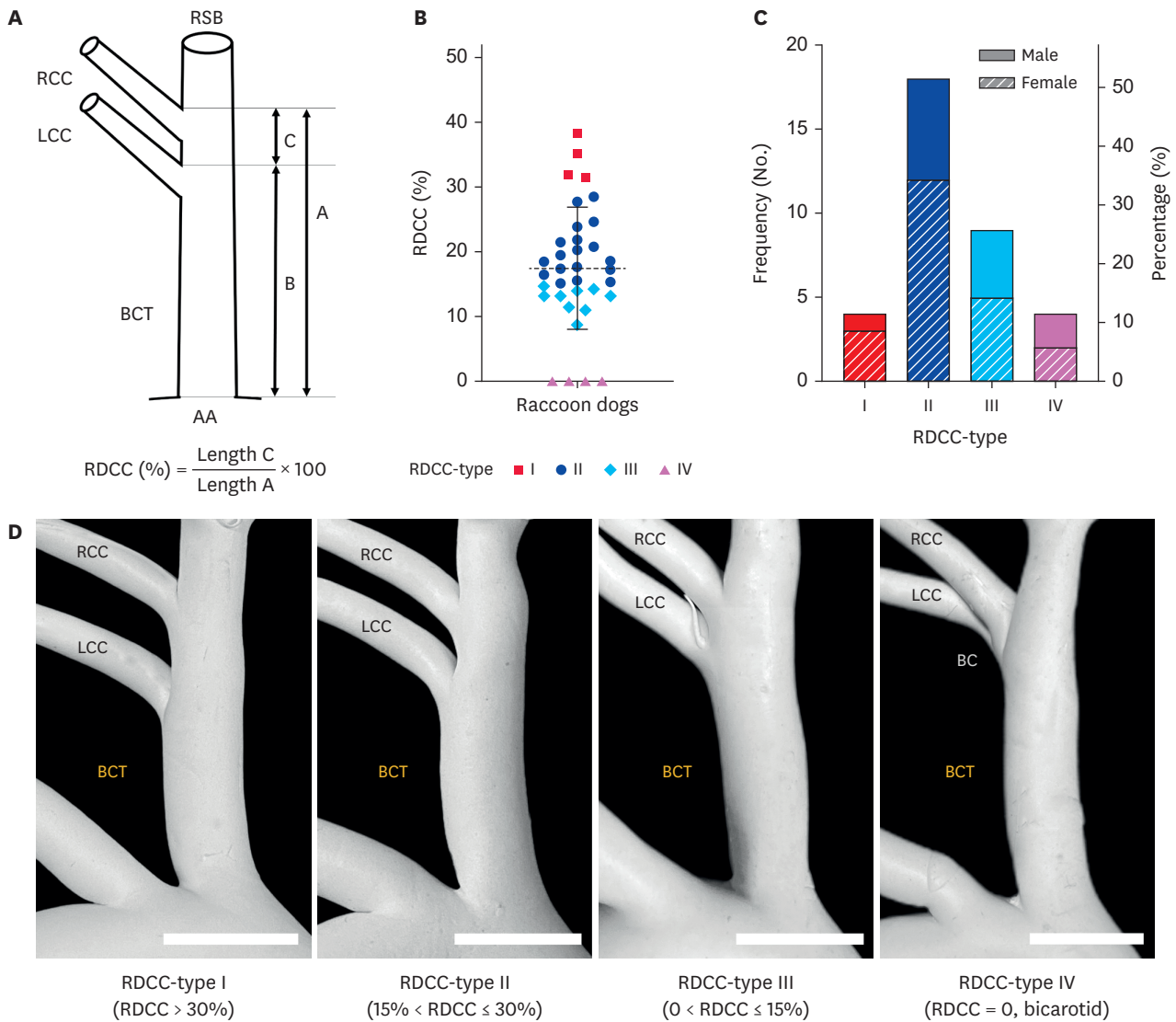


**Fig. 3.** Branching patterns of the BCT in raccoon dogs. (A) Schematic representation showing the measurement points for calculating RDCC. The figure represents the total length of the BCT (length A), the length from the AA to the LCC (length B), and the distance between LCC and RCC branches (length C). (B) The distribution of the RDCC in raccoon dogs. The dotted line indicates the mean, and the solid line indicates the SD. Each RDCC-type is symbolized as follows: square (■) for RDCC-type I, circle (●) for RDCC-type II, diamond (◆) for RDCC-type III and, triangle (▲) for RDCC-type IV. (C) The frequency of each RDCC-types of the BCT in the raccoon dog. Bars filled with solid color represent males, while those with diagonal stripes represent females. (D) Examples of silicone specimens representing each RDCC-type of the BCT. Scale bar = 10 mm.

AA, aortic arch; RSB, right subclavian artery; BCT, brachiocephalic trunk; LCC, left common carotid artery; RCC, right common carotid artery; RDCC, the ratio of the distance between the left and right common carotid arteries to the total length of the brachiocephalic trunk.

branched first in three (4.2%), followed by five (6.9%), 26 (36.1%), and 38 cases (52.8%), respectively. Statistical analyses revealed significant differences in the branching order of major SB arteries.

We also compared the branching order between LSB and RSB (**Fig. 6**). From the frequency distribution, it was evident that the VT and CCT predominantly branched as the first or second branches, whereas the SC and IT mainly branched as the third or fourth branches. Based on these observations, we grouped the data into first and second orders and third and fourth orders. A subsequent Mann-Whitney *U* test revealed that CCT showed statistically significant differences between LSB and RSB in the first and second orders ( $p = 0.038$ ). In addition, the

**Table 2.** Frequency of the branching types of the subclavian arteries in raccoon dogs

No.	SB-type	Arteries		Sex		Total (%)
		LSB	RSB	Female	Male	
1	VT-CCT-SC-IT	13	6	13	6	19 (26.4)
2	VT-CCT-[SC=IT]	7	3	7	3	10 (13.9)
3	VT-CCT-IT-SC	4	1	4	1	5 (6.9)
4	VT-CCT-IT≈SC	5	-	2	3	5 (6.9)
5	VT-[CCT=SC]-IT	-	4	3	1	4 (5.6)
6	VT≈CCT≈SC-IT	-	3	-	3	3 (4.2)
7	VT-[CCT=IT]-SC	2	1	3	-	3 (4.2)
8	[VT&CCT]-SC-IT	1	2	-	3	3 (4.2)
9	VT-CCT-SC≈IT	1	1	-	2	2 (2.8)
10	VT-CCT≈SC-IT	-	2	1	1	2 (2.8)
11	VT-CCT≈SC≈IT	-	1	-	1	1 (1.4)
12	[VT&CCT]-SC≈IT	-	1	-	1	1 (1.4)
13	[VT&CCT]-[SC=IT]	-	1	1	-	1 (1.4)
14	[VT&CCT]-IT-SC	1	-	1	-	1 (1.4)
15	[[VT&CCT]=IT]-SC	-	1	1	-	1 (1.4)
16	VT≈CCT-IT≈SC	-	1	1	-	1 (1.4)
17	VT≈CCT-[SC=IT]	-	1	1	-	1 (1.4)
18	[VT=CCT]-[SC=IT]	-	1	1	-	1 (1.4)
19	[VT=CCT]-SC-IT	-	1	1	-	1 (1.4)
20	[VT=CCT=IT]-SC	-	1	1	-	1 (1.4)
21	VT-CCT≈IT-SC	1	-	1	-	1 (1.4)
22	VT-[CCT=IT]≈SC	-	1	-	1	1 (1.4)
23	VT-SC≈CCT=IT	-	1	-	1	1 (1.4)
24	[VT=IT]-CCT-SC	1	-	1	-	1 (1.4)
25	VT-IT-CCT-SC	-	1	1	-	1 (1.4)
26	SC-[VT&CCT]-IT	-	1	-	1	1 (1.4)
	Total	36	36	44	28	72 (100)

SB, subclavian artery; LSB, left subclavian artery; RSB, right subclavian artery; VT, vertebral artery; CCT, costocervical trunk; IT, internal thoracic artery; SC, superficial cervical artery.

IT was statistically significant at the third and fourth positions ( $p = 0.021$ ). When considering all branching orders from the first to fourth, SC was found to be statistically significant ( $p = 0.012$ ). No differences in branching order were identified between sexes.

Based on our findings, the branching patterns of the four major SB arteries with frequencies exceeding 50% were as follows: VT branched first (98.6%), CCT branched second (81.9%), SC branched third (62.5%), and IT branched fourth (52.8%). Based on these results, the main branching pattern was determined to be VT-CCT-SC-IT (**Fig. 7A**).

We observed differences in the main branching patterns between LSB and RSB. For the LSB, the main branching pattern was VT-CCT-[SC=IT], with VT branching first (100%), CCT second (91.7%), and both SC and IT third (61.1% and 50.0%, respectively; **Fig. 7B**). In contrast, for the RSB, the main branching pattern was VT-CCT-SC-IT, with VT branching first (97.2%), CCT second (72.2%), SC third (63.9%), and IT fourth (63.9%) (**Fig. 7C**).

We investigated the symmetry of SB branching patterns between LSB and RSB (**Table 3**). Asymmetric cases were found in 29 animals (80.6%), while symmetric cases were found in only seven animals (19.4%).

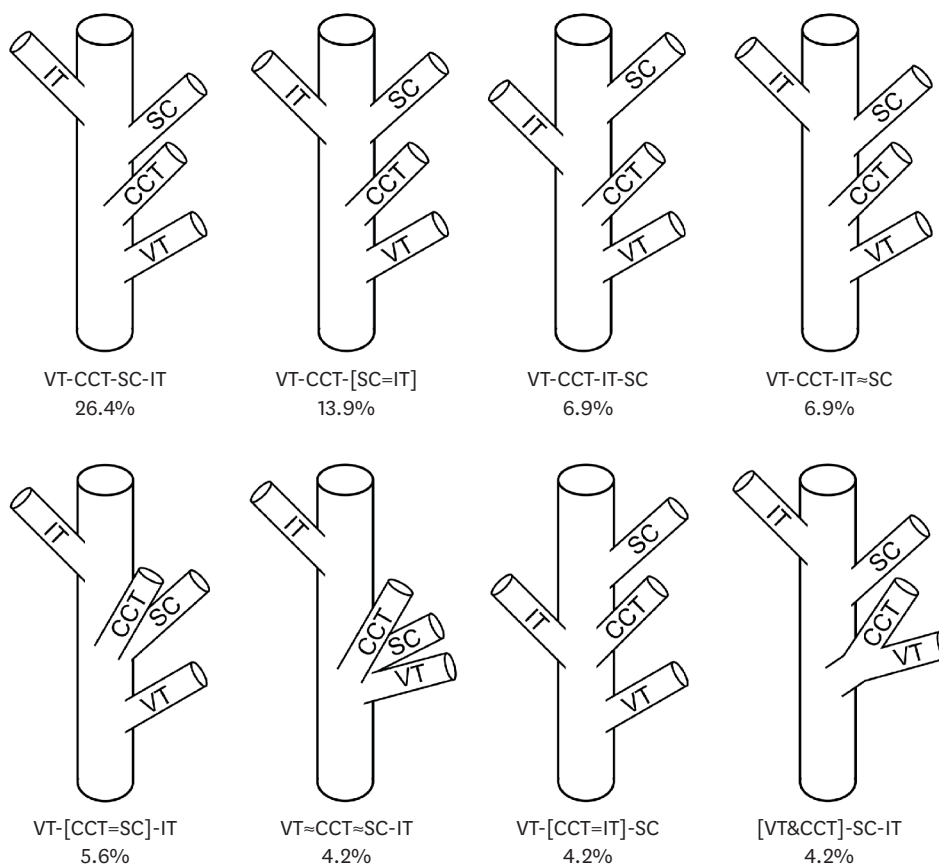


Fig. 4. Schematic diagrams illustrating the branching patterns of the subclavian artery in raccoon dogs, as observed in more than one case. VT, vertebral artery; CCT, costocervical trunk; SC, superficial cervical artery; IT, internal thoracic artery.

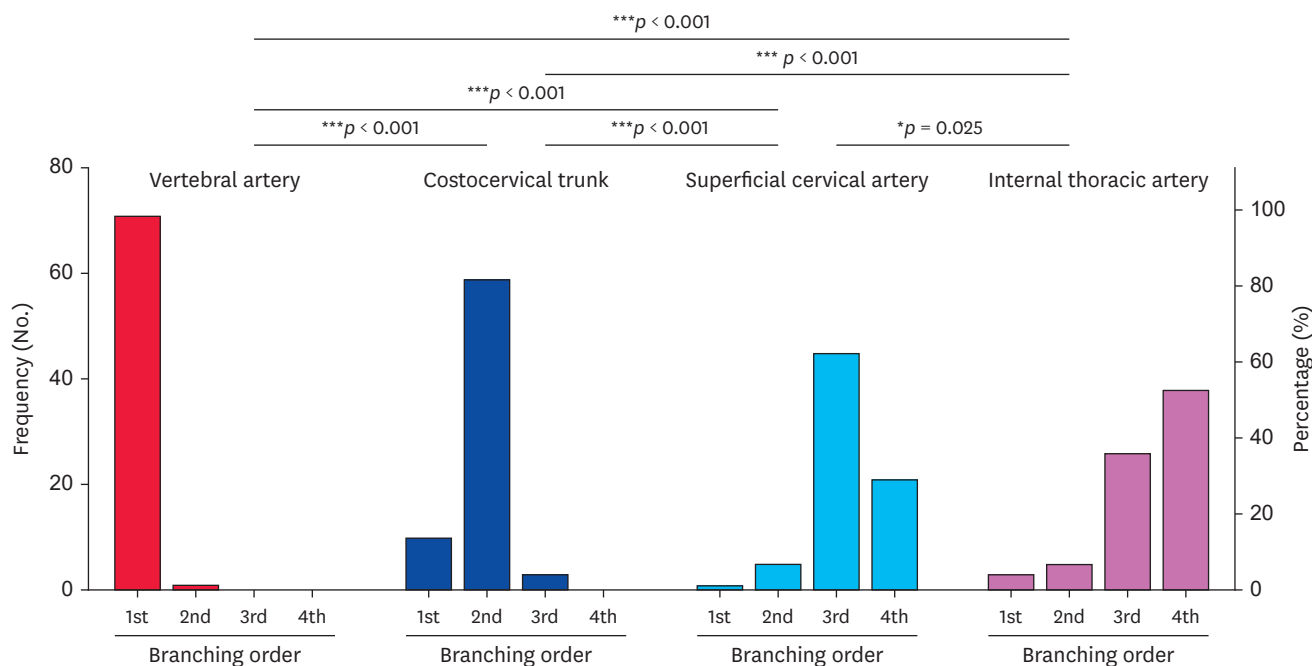
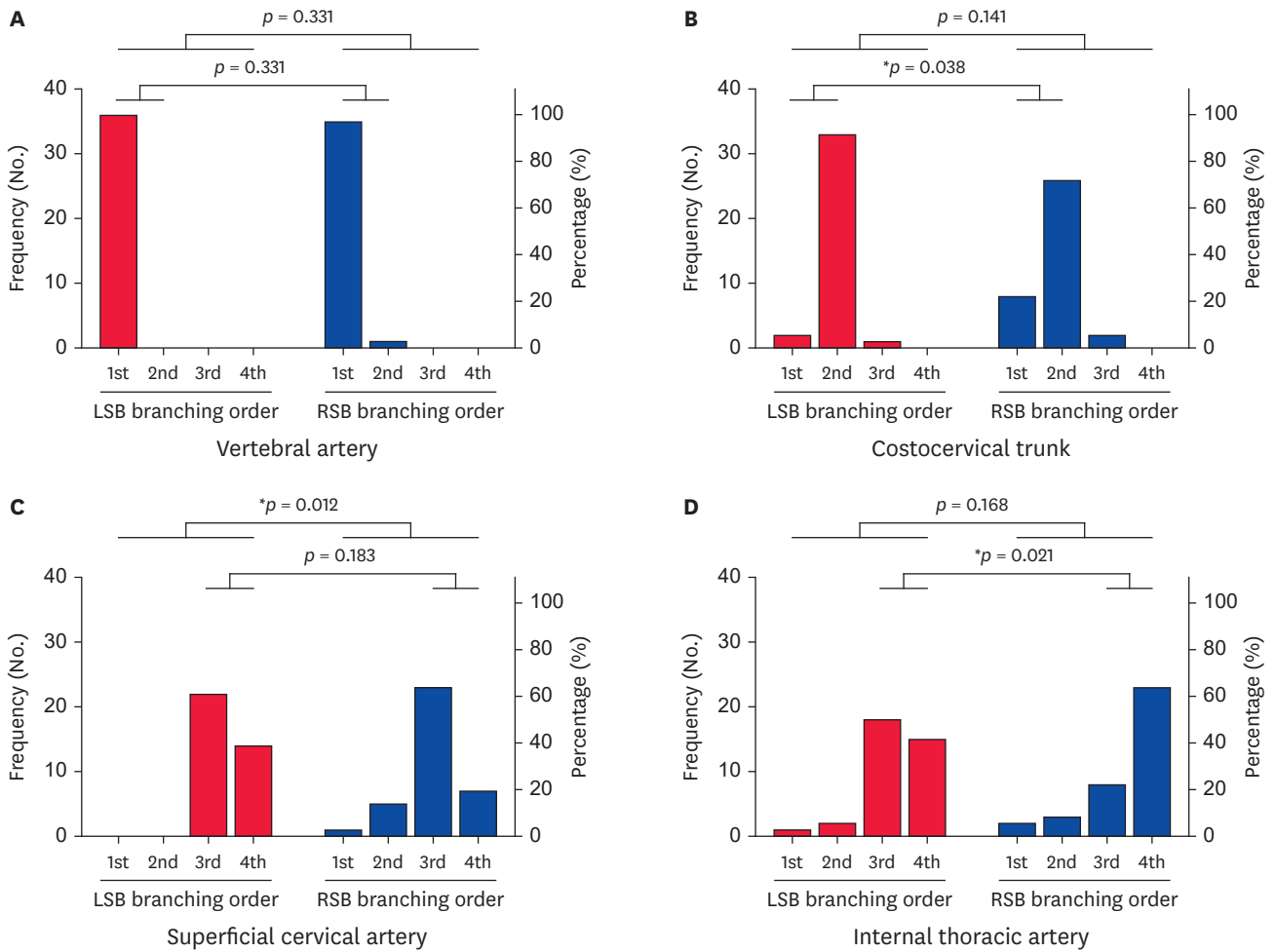
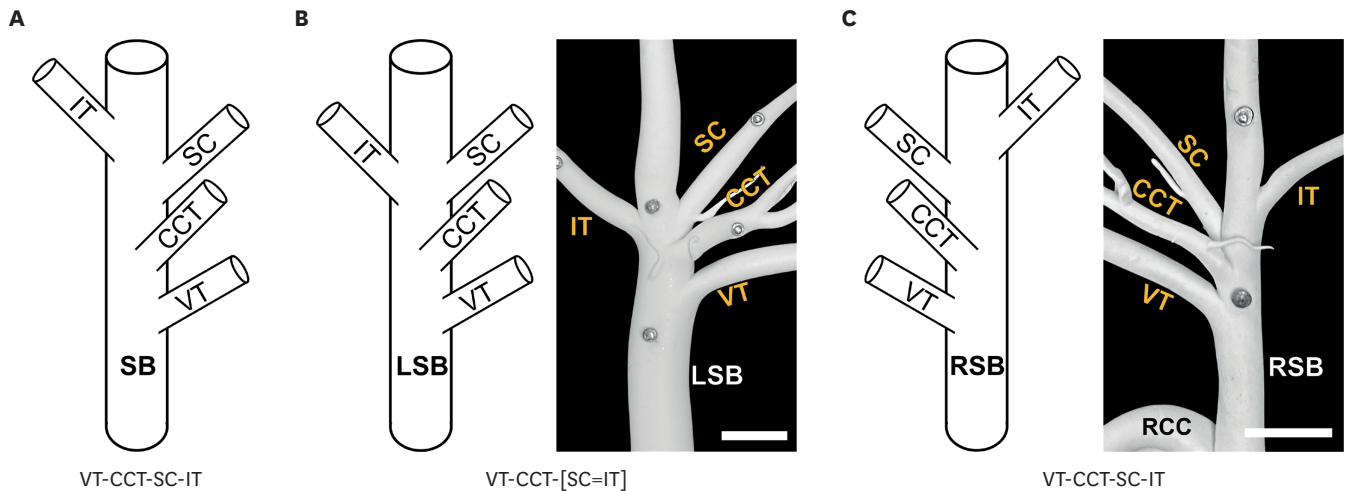


Fig. 5. Distribution of the branching order of each major branch of the subclavian artery in the raccoon dogs. Statistical analysis was performed using the Mann-Whitney *U* test. \**p* < 0.05; \*\*\**p* < 0.001.





**Fig. 6.** Distribution of the branching order of each major branch compared to left and right subclavian artery in raccoon dogs. Statistical analysis was performed using the Mann-Whitney *U* test. (A) Vertebral artery; (B) Costocervical trunk; (C) Superficial cervical artery; (D) Internal thoracic artery. LSB, left subclavian artery; RSB, right subclavian artery. \**p* < 0.05.



**Fig. 7.** The main branching pattern of the SB in raccoon dogs. (A) The main branching pattern of both the LSB and RSB. (B) The main branching pattern of the LSB. (C) The main branching pattern of the RSB. Scale bars, 10 mm. SB, subclavian artery; VT, vertebral artery; CCT, costocervical trunk; SC, superficial cervical artery; IT, internal thoracic artery; LSB, left subclavian artery; RSB, right subclavian artery; RCC, right common carotid artery.

**Table 3.** Frequency of symmetric or asymmetric branching patterns in the left and right subclavian arteries in the raccoon dogs

Sex	Symmetric cases (%)	Asymmetric cases (%)
Male (n = 14)	2 (14.3)	12 (85.7)
Female (n = 22)	5 (22.7)	17 (77.3)
Total (n = 36)	7 (19.4)	29 (80.6)

## DISCUSSION

The present study examined the morphology of AA branching patterns in raccoon dogs. We focused on three branching levels: AA, BCT, and SB. The morphology observed in raccoon dogs showed both similarities and differences with other carnivores.

The AA branching pattern varies among different animal species depending on the number of arteries branching from the AA. This variation is associated with thorax breadth [9,12]. For instance, animals with a laterally compressed thorax, such as ungulates (Bovidae [10], Equidae [8], and Cervidae [9]) usually exhibit AA-type I with only one artery: the BCT. Conversely, animals with a thorax compressed from dorsal to ventral, such as humans [36] and rhesus monkeys [6], commonly display AA-type III with three arteries: the BCT, LCC, and LSB.

Most carnivores with an intermediate thorax breadth predominantly exhibit AA-type II with two arteries: the BCT and LSB. These animals include dogs [20], cats [21], lions [12], Eurasian otters [2], foxes [22], raccoons [12], and tigers [12]. However, certain marine carnivores such as gray seals [12], deep-diving hooded seals [18], and ringed seals [19] have been reported to exhibit AA-type III. This suggests that marine habitats may influence branching patterns. In the present study, all 35 raccoon dogs exhibited AA-type II, aligning with the findings on most carnivores.

Previous investigations on BCT in carnivores have revealed intraspecific variations related to the configuration of LCC and RCC [20,21]. In the separation form, LCC and RCC branch individually. In the bifurcated form, they branch at the same point. In the bicarotid form, they form a common trunk known as the BC. In German shepherd dogs, the occurrences of the separation, bifurcation, and bicarotid forms were 50.0%, 21.7%, and 22.3%, respectively [20]. In cats, Gonzalez et al. [3] reported occurrences of 51.8%, 37.5%, and 10.7%, whereas Pongkan et al. [29] reported percentages of 63.3%, 31.7%, and 5.0%, respectively. The distributions of Eurasian otters were 76.7%, 27.8%, and 5.6%, respectively [2].

In our study, the BCT of raccoon dogs also showed intraspecific variation. The separation form was 62.8% for both RDCC-type I and II, the bifurcation form was 25.7% for RDCC-type III, and the bicarotid form was 11.4% for RDCC-type IV. Generally, in the BCT branching type in carnivores, the separation form was observed as a typical branching pattern in over 50% of the cases. The bifurcation and bicarotid forms were found to have anatomical intraspecific variations in a small proportion of dogs, cats, Eurasian otters, and raccoon dogs [2,3,20,21,29]. These findings suggest the potential for intraspecific variation in other unstudied carnivores.

For further investigation, we applied the RDCC, which is defined as the ratio of the distance between LCC and RCC to the total BCT length. This indicates the relative distance between the two arteries and suggests the degree of cranial fusion between the left and right third pharyngeal arch arteries during development [2,37]. In raccoon dogs, the incidence of RDCC

ranged from 0% to 38.3%, with an average of 17.5%. Based on the RDCC classification, RDCC-type II was the most common (51.4%). This suggests varied origins of LCC and RCC, depending on the animal. Furthermore, these findings indicate that cranial fusion occurred further from the BCT branching origin point but did not extend to the branching level of the fourth pharyngeal arch arteries [37]. In comparison, Eurasian otters exhibited an average RDCC of 20.0%, ranging from 0% to 31.6% [2]. This implies that the distance between LCC and RCC is generally shorter in raccoon dogs, although the distribution is more varied than that in Eurasian otters.

SB branching patterns vary significantly across species and individuals [1,2,24,625,29]. Although this diversity had long been unrecognized, recent studies in dogs [1,24,25], cats [29], and Eurasian otters [2] have revealed various branching patterns in the four arteries of the SB. Our study on raccoon dogs revealed 26 diverse branching patterns among individual animals.

Interspecific and intraspecific variability has caused inconsistent descriptions of the SB branching order in anatomical textbooks. Some textbooks, such as Nickel et al. [28], Ghoshal [27], and Hermanson et al. [17], state that VT branches first, followed by CCT; however, they do not specify the third branch. Singh stated that the order was VT first, CCT second, IT third, and SC fourth [35]. König et al. [16] stated CCT branching first, but did not specify the order of other arteries. Most textbooks do not specify the order of branches [13-15,26].

Furthermore, the interspecific variability in the SB branching pattern complicates the unified classification of various carnivores. In the conventional classification method of the SB branching pattern in dogs, Kim et al. [1] proposed a system with 12 branching types: four major types based on the branching order and level of the VT and CCT, and three subtypes based on those of the IT and SC. This classification has been proven effective for German shepherd dogs [1] and greyhounds [25]. However, as research expanded beyond dogs to other species, difficulties arose due to the various SB branching patterns. In studies on cats [29] and Eurasian otters [2], where the SB branched with the IT first or second, this classification was inapplicable. In our study of raccoon dogs, we encountered four exceptions in which this method could not be applied, specifically where the SC and IT branched either first or second (SB-types VT-SC≈CCT≈IT, [VT=IT]-CCT-SC, VT-IT-CCT-SC, and SC-[VT & CCT]-IT). To address these limitations, we applied a classification method based on the branching order of each SB arterial branch [2].

The SB branching patterns in raccoon dogs showed both similarities and differences. In dog breeds such as German shepherd dogs and greyhounds, VT branched first (99.1% and 97.0%, respectively), followed by CCT (75.9% and 52.5%, respectively) [1,25]. Similarly, in raccoon dogs, the VT branched first (98.6%) followed by the CCT (81.9%). This indicated a similarity between raccoon dogs and dogs, where the VT consistently appeared as the first branch followed by the CCT (VT-CCT).

However, the branching patterns of the IT and SC in the raccoon dogs were significantly different from those previously reported in the dogs [1,25]. In raccoon dogs, most cases showed that the SC branched third and the IT branched fourth (SC-IT). Such a pattern is not the predominant branching pattern in dogs. For instance, in German shepherd dogs, most cases represented the SC and IT branching together as the third branch ([SC=IT]) [1]. In greyhounds, most cases exhibited the opposite pattern, with SC branching third and IT branching last (IT-SC) [25].

These differences may have arisen from the variations in the shape of the thoracic cage [25]. Depending on the breed of dog, the thoracic cage can be classified based on the width-to-depth ratio into brachiomorphic (0.90 to 1.0), mesomorphic (0.60 to 0.89), and dolichomorphic groups (0.50 to 0.59) [38]. The German shepherd dog belongs to the mesomorphic group, whereas the greyhound belongs to the dolichomorphic group [38]. According to research on raccoon dogs, the width-to-depth ratio is 0.92, which falls within the brachiomorphic group [39]. Considering these facts, we suggest that the branching position of the IT branches becomes more cranial as the width-to-depth of the thoracic cage increase [25].

We also investigated the differences between LSB and RSB. The SB branching pattern was asymmetrical in most cases (80.6%). We identified statistical differences in the branching sequences of the CCT, SC, and IT between LSB and RSB. In particular, the most frequently observed branching order for the IT was third in the LSB and fourth in the RSB. Therefore, the main branching patterns differed between two sides: VT-CCT-[SC=IT] for the LSB, and VT-CCT-SC-IT for the RSB.

The differences between LSB and RSB may be attributed to their distinct embryological origins. Specifically, the proximal segment of the RSB originates from the right fourth AA artery, whereas the remainder is derived from the right dorsal aorta and right seventh dorsal intersegmental artery [37]. In contrast, the LSB originates from the seventh dorsal intersegmental artery, which emerges from the left dorsal aorta [37]. We assumed that these embryological differences could influence the branching differences between LSB and RSB.

In conclusion, raccoon dogs exhibited various branching patterns with both similarities and differences compared to other carnivores. We comprehensively described the AA branching patterns of raccoon dogs at three different levels: AA, BCT, and SB. In addition, this study provided a wide comparison with other carnivorous species. The AA and BCT branching patterns in raccoon dogs were similar to those observed in other carnivores; the AA branched into the BCT and LSB, and the BCT branched into LCC and RCC separately. However, in the SB branching pattern, most cases represented the SC branching third and the IT last, significantly differing from dogs.

## ACKNOWLEDGMENTS

The authors express their gratitude to the Jeonbuk Wildlife Rescue Center and Kangwon Wildlife Rescue Center for providing the raccoon dog carcasses.

## REFERENCES

1. Kim IS, Yang HH, Tae HJ, Na IJ, Leem HS, Ahn DC. Branching patterns of the subclavian arteries in German Shepherd dogs. *Anat Histol Embryol.* 2010;39(6):529-533. [PUBMED](#) | [CROSSREF](#)
2. Jang YJ, Sim J, Lee Y, Ahn D. Morphology of aortic arch branching patterns in the Eurasian Otter (*Lutra lutra*, Linnaeus, 1758). *J Vet Med Sci.* 2023;85(4):399-406. [PUBMED](#) | [CROSSREF](#)
3. Gonzalez VH, Ball S, Cramer R, Smith A. Anatomical and morphometric variations in the arterial system of the domestic cat. *Anat Histol Embryol.* 2015;44(6):428-432. [PUBMED](#) | [CROSSREF](#)
4. Oliveira RE, Araújo Júnior HN, Costa HS, Oliveira GB, Moura CE, Oliveira DJ, et al. Collateral arteries of the aortic arch in Mongolian gerbil (*Meriones unguiculatus*). *Acta Sci Vet.* 2018;46(1):8. [CROSSREF](#)

5. Nourinezhad J, Ranjbar R, Rostamizadeh V, Tabrizinejad MN, Hallak A, Janeczek M. Morphology of the pattern of branching of the aortic arch (Arcus aortae) in Syrian hamsters (*Mesocricetus auratus*). *Vet Res Commun.* 2023;47(1):51-60. [PUBMED](#) | [CROSSREF](#)
6. Garis CF. Branches of the aortic arch in 153 rhesus monkeys (second series). *Anat Rec.* 1938;70(3):251-262. [CROSSREF](#)
7. Ghoshal NG. Porcine heart and arteries. In: Getty R, editor. *Sisson and Grossman's the Anatomy of the Domestic Animals*. 5th ed. Philadelphia: W.B. Saunders; 1975, 1036-1042.
8. Ghoshal NG. Equine heart and arteries. In: Getty R, editor. *Sisson and Grossman's the Anatomy of the Domestic Animals*. 5th ed. Philadelphia: W.B. Saunders; 1975, 554-618.
9. Ahn DC, Kim HC, Tae HJ, Kang HS, Kim NS, Park SY, et al. Branching pattern of aortic arch in the Korean water deer. *J Vet Med Sci.* 2008;70(10):1051-1055. [PUBMED](#) | [CROSSREF](#)
10. Ghoshal NG. Ruminant heart and arteries. In: Getty R, editor. *Sisson and Grossman's the Anatomy of the Domestic Animals*. 5th ed. Philadelphia: W.B. Saunders; 1975, 960-1023.
11. Al Aiyan A, Balan R. Mapping the branching pattern of the middle cerebral artery in the camel (*Camelus dromedarius*): a comprehensive anatomical analysis. *Front Vet Sci.* 2023;10:1224197. [PUBMED](#) | [CROSSREF](#)
12. Parsons FG. On the arrangement of the branches of the mammalian aortic arch. *J Anat Physiol.* 1902;36(Pt 4):389-399. [PUBMED](#)
13. Smith BJ. *Canine Anatomy*. 1st ed. Philadelphia: Lippincott Williams & Wilkins; 1999, 349-357.
14. Pasquini C, Spurgeon T, Pasquini S. *Anatomy of Domestic Animals: Systemic and Regional Approach*. 10th ed. Pilot Point: Sudz Publishing; 2003, 408-421.
15. Adams DR. *Canine Anatomy: A Systemic Study*. 4th ed. Iowa: Iowa State Press; 2004, 267-298.
16. König HE, Ruberte J, Liebich HG. Organs of the cardiovascular system (systema cardiovasculare). In: König HE, Liebich HG, editors. *Veterinary Anatomy of Domestic Mammals: Textbook and Colour Atlas*. 7th ed. Stuttgart: Georg Thieme Verlag; 2020, 471-500
17. Hermanson JW, de Lahunta A, Evans HE. *Miller and Evans' Anatomy of the Dog*. 5th ed. St. Louis: Elsevier Saunders; 2020, 495-581.
18. Drabek CM, Burns JM. Heart and aorta morphology of the deep-diving hooded seal (*Cystophora cristata*). *Can J Zool.* 2002;80(11):2030-2036. [CROSSREF](#)
19. Smodlaka H, Henry RW, Reed RB. Macroscopic anatomy of the great vessels and structures associated with the heart of the ringed seal (*Pusa hispida*). *Anat Histol Embryol.* 2009;38(3):161-168. [PUBMED](#) | [CROSSREF](#)
20. Ahn DC, Tae HJ, Kim IS. Morphological patterns of the origin of the common carotid artery in German shepherd dogs. *Indian Vet J.* 2010;87(6):587-590.
21. More S, Watson A, Stein LE. Bicarotid trunk in the domestic cat. *Anat Histol Embryol.* 2016;45(5):350-356. [PUBMED](#) | [CROSSREF](#)
22. Lima AR, Souza DC, Carmo DC, Santos JT, Branco É. Ramos colaterais do arco aórtico e suas principais ramificações no cachorro-do-mato (*Cerdocyon thous*). *Pesqui Vet Bras.* 2016;36(7):647-651. [CROSSREF](#)
23. Raven HC. Notes on the anatomy of the viscera of the giant panda (*Ailuropoda melanoleuca*). *Am Mus Novit.* 1936;877:1-23.
24. Chawangwongsanukun R, Darawiroj D, Wongtawan T. New branching patterns of the subclavian arteries found in Thai native dogs. *J Appl Anim Sci.* 2019;12(3):41-55.
25. Pols S, Henneberg M, Norris R. Cranial arterial patterning in greyhounds: another case of internal intraspecific variation. *Anat Histol Embryol.* 2016;45(3):161-172. [PUBMED](#) | [CROSSREF](#)
26. Budras KD, McCarthy PH, Fricke W, Richter R. *Anatomy of the Dog*. 5th ed. Hannover: Schlütersche; 2007, 38-49.
27. Ghoshal NG. Carnivore heart and arteries. In: Getty R, editor. *Sisson and Grossman's the Anatomy of the Domestic Animals*. 5th ed. Philadelphia: W.B. Saunders; 1975, 1594-1651.
28. Nickel R, Schummer A, Seiferle E. *The Anatomy of the Domestic Animals, Vol. 3, the Circulatory System, the Skin, and the Cutaneous Organs of the Domestic Mammals*. 1st ed. Berlin and Hamburg: Verlag Paul Parey; 1981, 71-77.
29. Pongkan W, Banjongkankul W, Ketyungyuenwong P, Kongtueng P, Buddhachat K, Nganvongpanit K. New findings of branching variations in subclavian arteries and supra-aortic arteries in *Felis catus*. *Anat Sci Int.* 2020;95(4):440-454. [PUBMED](#) | [CROSSREF](#)
30. Sun W, Yang Y, Li GY. The complete mitochondrial genome of the raccoon dogs (Canidae: *Nyctereutes ussuriensis*) and intraspecific comparison of three Asian raccoon dogs. *Mitochondrial DNA B Resour.* 2019;4(1):670-671. [CROSSREF](#)
31. Hong Y, Lee H, Kim KS, Min MS. Phylogenetic relationships between different raccoon dog (*Nyctereutes procyonoides*) populations based on four nuclear and Y genes. *Genes Genomics.* 2020;42(9):1075-1085. [PUBMED](#) | [CROSSREF](#)

32. Brudnicki W, Wiland C, Jabłoński R. Basilar arteries of the brain in raccoon dog (*Nyctereutes procyonoides* (Gray, 1834)). Arch Vet Pol. 1994;34(1-2):141-147. [PUBMED](#)
33. Fujiwara S, Suwa F. On the facial artery of the raccoon dog (*Nyctereutes procyonoides viverrinus* Temminck). Okajimas Folia Anat Jpn. 1991;68(2-3):81-93. [PUBMED](#) | [CROSSREF](#)
34. Skoczylas B, Brudnicki W, Kirkiłło-Stacewicz K, Nowicki W, Wach J. Telencephalon vascularity in raccoon dog (*Nyctereutes procyonoides* Grey 1834). Electron J Pol Agric Univ. 2015;18(1):4.
35. Singh B. The thorax of the dog and cat. In: Singh B, editor. *Dyce, Sack, and Wensing's Textbook of Veterinary Anatomy*. 5th ed. St. Louis: Elsevier Saunders; 2018, 403-417.
36. De Garis CF, Black IH, Riemenschneider EA. Patterns of the aortic arch in American white and negro stocks, with comparative notes on certain other mammals. J Anat. 1933;67(Pt 4):599-619. [PUBMED](#)
37. McGeady TA, Quinn PJ, Fitzpatrick ES, Ryan MT, Kilroy D, Lonergan P. *Veterinary Embryology*. 2nd ed. Chichester: Wiley Blackwell; 2017, 119-147.
38. Santilli RA, Porteiro Vázquez DM, Gerou-Ferriani M, Lombardo SF, Perego M. Development and assessment of a novel precordial lead system for accurate detection of right atrial and ventricular depolarization in dogs with various thoracic conformations. Am J Vet Res. 2019;80(4):358-368. [PUBMED](#) | [CROSSREF](#)
39. Ahn S, Lee M, Shin W, Han Y, Bae S, Choi SY, et al. Radiographic measurement of vertebral heart scale in Korean wild raccoon dogs (*Nyctereutes procyonoides koreensis*). J Zoo Wildl Med. 2023;53(4):817-822. [PUBMED](#) | [CROSSREF](#)